Magnetic field switching of the charge-density-wave state in the lanthanide intermetallic SmNiC$_2$

N. Hanasaki

Department of Physics, Osaka University, Toyonaka 560-0043, Japan

Y. Nogami and M. Kakinuma

Department of Physics, Okayama University, Okayama 700-8530, Japan

S. Shimomura

Department of Physics, Kyoto Sangyo University, Kyoto 603-8555, Japan

M. Kosaka

Department of Physics, Saitama University, Saitama 338-8570, Japan

H. Onodera

Institute for Materials Research, Tohoku University, Sendai 980-8577, Japan

In the intermetallic SmNiC$_2$, the ferromagnetic metallic state competes with the charge-density-wave state. We can switch the charge-density-wave state by applying a magnetic field that is conjugated to the magnetization of the order parameter in the ferromagnetic state, and show the giant negative magnetoresistance. Under the applied magnetic field, the resistivity becomes one order of magnitude smaller than the zero-field resistivity.

The interactions cause the order formation in the electron systems.[1,2] In the second-order phase transition, the short-range correlation grows just above the critical temperature. The susceptibility of the order parameter for the external conjugated field is enhanced. In the first-order transition, the jump in the order parameter and the physical properties is expected owing to a finite potential barrier between the minima in the free energy. When different phases with independent order parameters touch in the phase diagram, the first-order transition will occur in the boundary, in which two kinds of the potential minima exist. In this way, phase competition can cause a gigantic response to an external stimulus by use of the first-order type nature. For example, in manganese oxides, the ferromagnetic metallic (FMM) state competes keenly with an antiferromagnetic charge-orbital-ordered (CO) state.[3–5] The magnetic field conjugated to the magnetization of the FMM order parameter can switch the highly resistive CO into metallic states. With the success of these oxides, experimental studies to produce the gigantic response tend to focus on the transition-metal oxides, which possess the Hund coupling between the conduction electron and the local moment.

In the lanthanide intermetallics having a Kondo coupling such as Gd$_5$(Si$_x$Ge$_{1-x}$)$_4$, large magnetoresistance is observed near the metamagnetic transition between the antiferromagnetic (AF) state and the forced ferromagnetic state.[6–8] Nevertheless, the reported magnetoresistance ratio $|\Delta\rho/\rho|$ is at most ∼0.4. This is because the exchange interaction due to hybridization between the f electron and the conduction electron is not strong in these systems. Another way to produce a gigantic response is to apply the phase competition associated with the highly resistive state. The intermetallic compound SmNiC$_2$ undergoes the charge-density-wave

(CDW) state and the FMM state at low temperatures.[9,10] The order parameter of the CDW state is an independent parameter of the magnetization characteristic to the FM state. In this Brief Report, we use this phase competition to demonstrate the magnetic-field switching of the CDW state, and report its resultant giant magnetoresistance in SmNiC$_2$. Here, the CDW state, having a high transition temperature of 150 K, can be completely suppressed by the low magnetic field of a few Tesla. It is known that, in actinide intermetallics such as uranium compounds, large magnetoresistance is seen at the metamagnetic transition as well.[11,12] However, the underlying mechanism is quite different from that in the present compound, since the magnetoresistance is ascribed to the magnetic reconstruction of the Fermi surface induced by the metamagnetic transition.[13,14]

The inset of Fig. 1(a) displays the crystal structure of SmNiC$_2$. The structure belongs to an orthorhombic system with the space group *Amm*2: $a = 3.7037(3)$ Å, $b = 4.5279(2)$ Å, and $c = 6.0947(4)$ Å.[15] The Sm, Ni, and C$_2$ atoms form uniform chains along the a axis. The Sm and Ni chains make a quasitriangular lattice within the bc plane. Since the triangles of the Ni and C$_2$ atoms are oriented in the opposite direction, there is no space inversion symmetry. According to the band calculations, the density of states (DOS) at the Fermi level consists of the Sm $5d$, Ni $3d$, and O $2p$ orbital components. The predicted Fermi surface has warping sheets parallel to the bc plane.[16] The DOS at the Fermi level does not contain the Sm $4f$ component, suggesting that the $4f$ orbital has the character of the local moment.

Figure 1 depicts a comparative plot of the magnetization (a), resistivity (b), and x-ray diffraction (c) in SmNiC$_2$. The resistivity slightly increases below 150 K, as indicated by the vertical bar ($T_{\rm CDW}$) on the bottom abscissa, and the
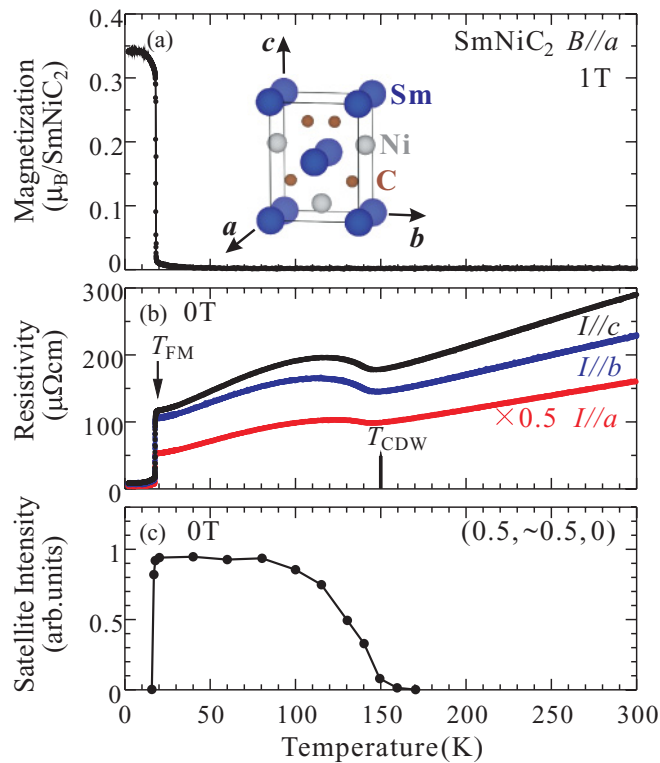
FIG. 1. (Color online) Temperature dependence of various quantities in SmNiC$_2$. (a) Magnetization at $B = 1$ T along the a axis. Inset: Crystal structure of SmNiC$_2$. (b) Resistivity measured under the current applied along the a axis (red), the b axis (blue), and the c axis (black). The FM transition temperature (T_{FM}) and the CDW transition temperature (T_{CDW}) are indicated by the arrow and the thick vertical bar on the bottom abscissa, respectively. (c) Integrated intensity of the satellite peak at (0.5, ~0.5, 0) in the x-ray diffraction, which was also reported in the preceding paper (Ref. 10).

x-ray satellite peak intensity grows.[10] The wave number of (0.5, ~0.5, 0) in the satellite peak is consistent with the nesting vector of the sheetlike Fermi surface predicted by the band calculations, indicating the formation of the CDW state.[16] According to a previous report, when the temperature decreases the b^* component of the satellite continuously changes in the region between 0.49 and 0.52.[10] The intensity of the satellite peak is one or two orders of magnitude weaker than the intensity of the Bragg reflections, suggesting that the satellite peak is mainly ascribable to the periodic lattice distortion of the Sm and Ni atoms, as reported by Wölfel et al.[15] The gap formation due to the CDW is also observed in the photoemission spectra.[17] Below 110 K, the resistivity starts to decrease, since part of the Fermi surface survives probably owing to the imperfect nesting of the CDW. Near $T_{FM} \approx 17.7$ K, the resistivity drops drastically. The satellite peaks disappear as well, indicating the complete suppression of the CDW state and its resultant resurrection of the DOS at the Fermi level. The magnetization is enhanced drastically and saturated below T_{FM}.[9] Thus, this FM transition accompanied by the suppression of the CDW indicates the phase competition between the CDW and FMM states.

Single crystals of SmNiC$_2$ were obtained by use of a tetra arc furnace in Ar gas.[9] The resistivity and magnetization

are measured by the Quantum Design physical property measurement system. To detect an x-ray diffraction signal under a high magnetic field up to 10 T, we used the JASTEC JMTXD-1010NA liquid-helium-free superconducting magnet with a large room-temperature bore (100 mmϕ). With the help of this windowless bore, x-ray radiation can pass freely in the magnetic field without diffraction noise from the magnet window. In that bore, we inserted an XR-CS10K low-noise fixed IP (imaging plate) camera (Japan Thermal Engineering Ltd.,) cooled by a continuous helium flow, in which the sample crystal is fixed. The Mo Kα radiation from the Ru-450 low-voltage rotating-anode x-ray generator (Rigaku Ltd.) was focused and monochromatized by a bent HOPG (highly oriented pyrolytic graphite). Owing to the angular divergence of the focused beam, we obtained oscillation photographs without rotating the sample crystal. The x-ray voltage is always less than 32 kV so as not to generate harmful $\lambda/2$ contamination, which may add the extra Bragg reflection of $\lambda/2$ at the midpoint of the Bragg reflection of λ. This extra reflection resembles that for the modulated crystal that contains both the Bragg and satellite spots of λ. The typical tube current and exposure time are 180 mA and 6 min, respectively.
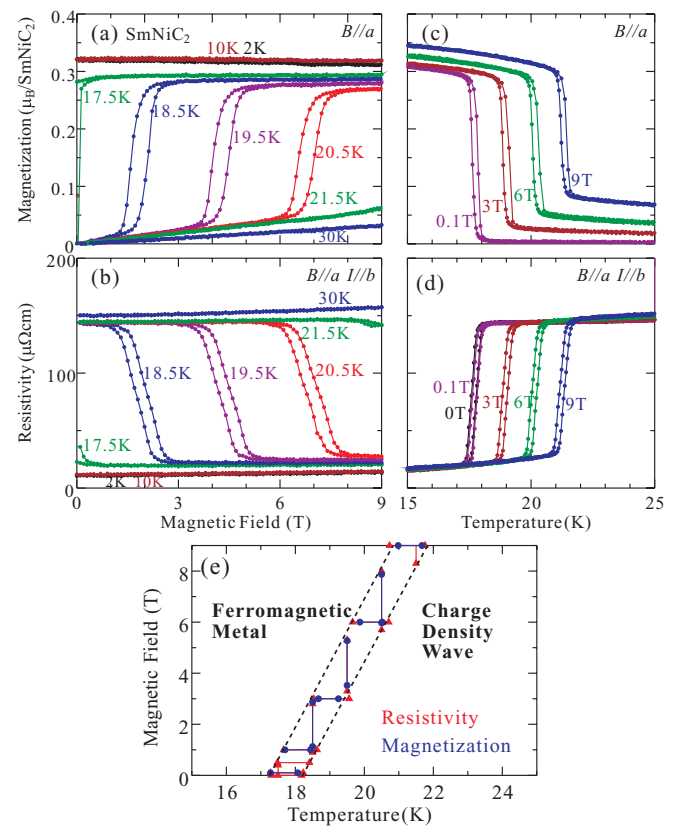

FIG. 2. (Color online) Magnetic-field dependence of the magnetization (a) and resistivity (b) at $T = 2, 10, 17.5, 18.5, 19.5, 20.5, 21.5,$ and 30 K in SmNiC$_2$. The magnetic field and the current are applied along the a and b axes, respectively. The temperature dependence of the magnetization (c) and the resistivity (d) near the FM transition under the magnetic field of $B = 0, 0.1, 3, 6,$ and 9 T. (e) Phase diagram of the FMM and CDW states, which are derived from the resistivity (red triangles) and magnetization (blue circles). The hysteresis region exists between the dashed black lines.
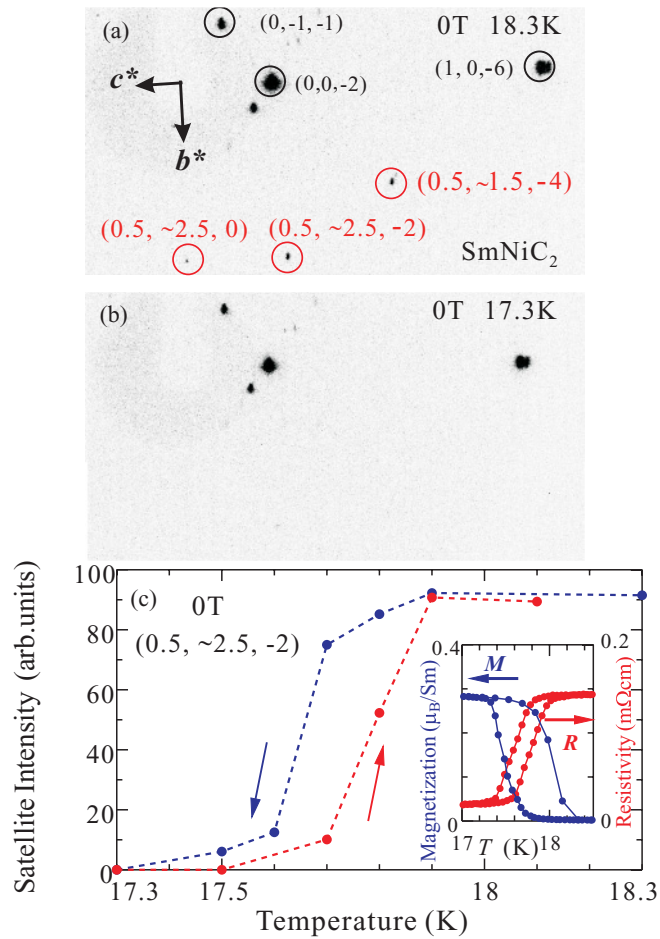
FIG. 3. (Color online) X-ray diffraction photographs at $T =$ 18.3 K (a) and 17.3 K (b) in the absence of a magnetic field in SmNiC$_2$. The red circles indicate the satellite peaks at (0.5, ∼2.5, 0), (0.5, ∼2.5, −2), and (0.5, ∼1.5, −4), and the black circles indicate the Bragg reflections. (c) Temperature dependence of the integrated intensity in the satellite peak at (0.5, ∼2.5, −2) during the cooling (blue) and heating (red) processes. Inset: Resistivity (red) in $B = 0$ T and magnetization (blue) in $B = 0.1$ T. The current and the magnetic field are applied along the b and a axes, respectively.

The magnetic-field-temperature phase diagram is investigated in detail near the FM transition.[9] Figures 2(a) and 2(b) show the magnetic-field dependence of the magnetization and resistivity, respectively. When the magnetic-field strength is increased, the magnetization is enhanced drastically at the transition with the hysteresis width of about 2 T. Under the magnetic field, the resistivity becomes one order of magnitude smaller than the zero-field resistivity. The magnetic fields in which resistivity suddenly drops coincide closely with those in which magnetization is enhanced. The reduction of resistivity is accompanied by the ferromagnetic transition. When the temperature increases, the critical field shifts toward the higher fields. Whereas in the CDW phase (for example, 30 K) the magnetization increases with the magnetic-field strength, the increment of the resistivity with the magnetic field is slightly positive. This reveals that the contribution of spin scattering to resistivity is negligible.

We display the temperature dependence of the magnetization in Fig. 2(c). One can see the clear hump of the magnetization near 17.7 K and its hysteresis, whose width is about 1 K, indicating the first-order nature of this transition. The magnetic field shifts the transition temperature toward the higher region, owing to the stabilization of the ferromagnetic state. Figure 2(d) shows that the resistivity drop is accompanied by the magnetization enhancement. The hysteresis width of the resistivity is slightly wider than that of
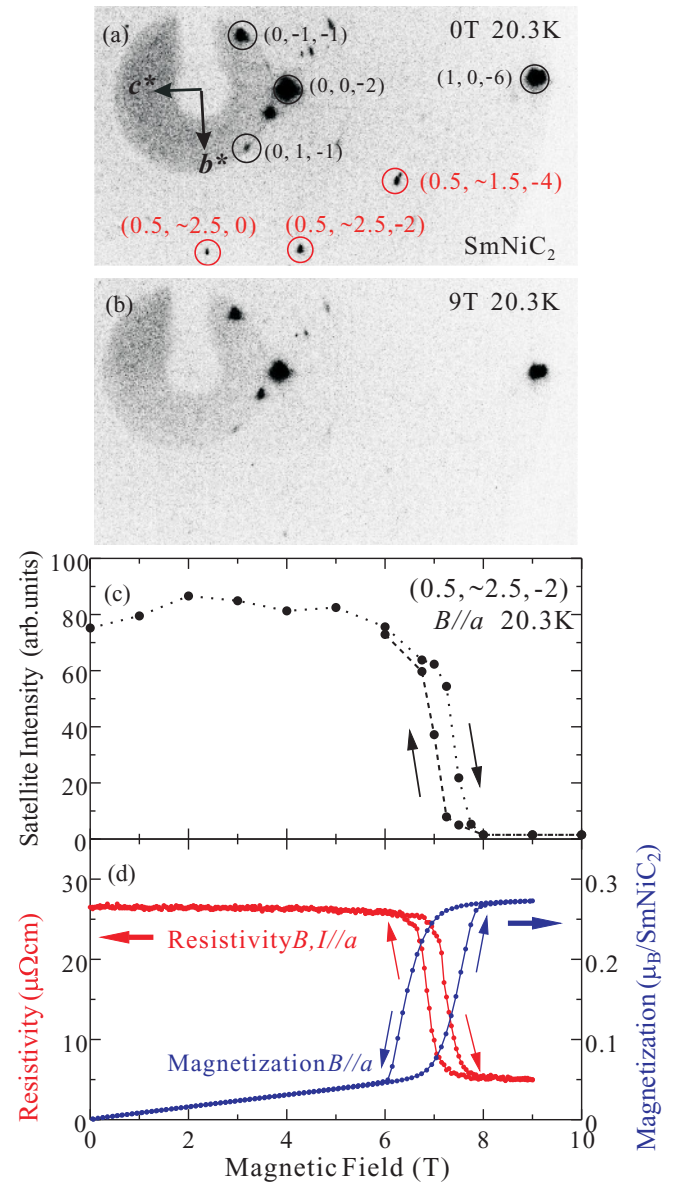

FIG. 4. (Color online) X-ray diffraction photographs in $B =$ 0 T (a) and 9 T (b) applied along the a axis at $T = 20.3$ K in SmNiC$_2$. The red circles indicate the satellite peaks at (0.5, ∼2.5, 0), (0.5, ∼2.5, −2), and (0.5, ∼1.5, −4), and the black circles indicate the Bragg reflections. (c) Magnetic-field dependence of the integrated intensity in the satellite peak at (0.5, ∼2.5, −2) at $T = 20.3$ K. (d) The magnetic-field dependence of the resistivity (red) and the magnetization (blue). Both the magnetic field and the current are applied along the a axis.

the magnetization, since the electric conductivity is sensitive to the small volume fraction of the low-resistive FMM domains in the CDW state. Recently, Laverock *et al.* calculated the Fermi surface and the susceptibility of the Peierls instability in $SmNiC_2$.[16] This susceptibility peak becomes gradual in the ferromagnetic state, indicating the magnetic-field-induced suppression of the CDW. The saturated magnetization $M = 0.34\mu_B/SmNiC_2$ is smaller than the expected Sm moment ($0.7\,\mu_B/Sm$). The magnetic circular dichroism (MCD) spectra reveal spin polarization not only in the Sm $5d$ moment but also in the Ni moment.[18] Since the DOS peaks near the Fermi level according to the band calculation,[16] one possible origin of this FMM state is the exchange interaction in the Stoner model, leading to the spin polarization of the conducting d electron. Owing to the J_{cf} interaction between the Sm $4f$ moment and the conducting d electrons of the Ni and Sm, the $4f$ moments are also aligned so as to produce the FMM state. Figure 2(e) depicts the phase diagram studied by the magnetization (blue circles) and the resistivity (red triangles). Here, the bars indicate the hysteresis region of the transition. The transition temperature is shifted at the ratio of 0.3 K/T. It is possible to switch the CDW state by applying the magnetic field at $T = 18.2 \sim 20.7$ K.

Let us discuss the relationship between the crystal structure and the phase transition. Figures 3(a) and 3(b) display the x-ray diffraction photographs at 18.3 K and 17.3 K in the absence of a magnetic field, respectively. Here, the direction of the x-ray incident beam is nearly parallel to the a axis. The IP is set in the plane perpendicular to the a axis. The arrows indicate the direction of the reciprocal vectors of the b^* and c^* axes. The starting point of these vectors corresponds to the position that the direct x-ray beam passes; in other words, reciprocal lattice origin (Γ point). In Fig. 3(a), one can find the satellite peaks due to the CDW indicated by the red circles and their indices, besides the Bragg reflections indicated by the black circles. As shown in Fig. 3(b), the satellite peaks disappear as the temperature decreases, indicating the suppression of the CDW state. Figure 3(c) displays the temperature dependence of the intensity in the satellite peaks at (0.5, ~2.5, −2). As the temperature decreases, the intensity of the satellite peak decreases drastically near 17.7 K. The hysteresis in the satellite intensity is also clear in the transition region, which is in agreement with the FM transition shown in the inset.

Figure 4 displays the magnetic-field effect of the satellite peaks at 20.3 K. In the x-ray diffraction photographs, the red circles indicate the satellite peaks. As shown in Fig. 4(b),

the CDW satellite peaks disappear under the magnetic field of 9 T applied along the a axis, indicating the magnetic-field-induced suppression of the CDW. Figure 4(c) shows the magnetic-field dependence of the intensity in the satellite peak at (0.5, ~2.5, −2). One can see the remarkable reduction in the peak intensity and its hysteresis near 7 T. The change in x-ray diffraction is fully consistent with those in the resistivity and the magnetization of the macroscopic measurement, as displayed in Fig. 4(d). The magnetic field where the phase transition occurs is also in accord with the phase diagram in Fig. 2(e). Figure 4(c) gives microscopic evidence that the resistivity reduction comes from the magnetic-field-induced suppression of the CDW state.

The CDW state competes with the FMM state. In the former, the DOS at E_F is reduced, owing to the partial nesting of the Fermi surface. On the other hand, in the latter the d band is polarized, accompanying the ferromagnetic arrangement of the f moments. The spin polarization, in which the major (minor) spin band is shifted toward the lower (higher) energy, causes the deviation of the Fermi wave number from the nesting condition of the CDW.[16] By applying the magnetic field, the energy of the FMM state becomes low compared with that of the CDW state. Thus, the CDW state is suppressed and the DOS at the Fermi level is resurrected, leading to the giant magnetoresistance.

In summary, we present another mechanism of giant magnetoresistance in the lanthanide f electron system through the investigation of the magnetic-field-temperature phase diagram of the CDW and FMM states. The phase transition between these states has the first-order character. We also demonstrate the magnetic-field switching of the CDW state. The resistivity becomes one order of magnitude smaller than the zero-field resistance. We expect that the gigantic response produced by the phase control will contribute to new research topics in the interesting f electron physics. Not only the magnetic field but also the pressure are the important parameters controlling the phase transition.

---

[1] W. Gebhardt and U. Krey, *Phasenübergänge und kritische Phänomene* (Friedr. Vieweg and Sohn, Braunschweig/Wiesbaden, 1980).

[2] H. E. Stanley, *Introduction to phase transitions and critical phenomena* (Oxford University Press, Oxford, 1987).

[3] Y. Tokura and N. Nagaosa, Science **288**, 462 (2000).

[4] A. Asamitsu, Y. Moritomo, Y. Tomioka, T. Arima, and Y. Tokura, Nature (London) **373**, 407 (1995).

[5] Y. Tomioka and Y. Tokura, Phys. Rev. B **66**, 104416 (2002).

[6] V. K. Pecharsky and K. A. Gschneidner Jr., Adv. Mater. **13**, 683 (2001).

[7] H. P. Kunkel, X. Z. Zhou, P. A. Stampe, J. A. Cowen, and G. Williams, Phys. Rev. B **53**, 15099 (1996).

[8] J. Y. Chan, S. M. Kauzlarich, P. Klavins, R. N. Shelton, and D. J. Webb, Chem. Mater. **9**, 3132 (1997).

[9] H. Onodera, Y. Koshikawa, M. Kosaka, M. Ohashi, H. Yamauchi, and Y. Yamaguchi, J. Magn. Magn. Mater. **182**, 161 (1998).

[10] S. Shimomura, C. Hayashi, G. Asaka, N. Wakabayashi, M. Mizumaki, and H. Onodera, Phys. Rev. Lett. **102**, 076404 (2009).

[11]V. Sechovský, L. Havela, K. Prokeš, H. Nakotte, F. R. de Boer, and E. Brück, J. Appl. Phys. **76**, 6913 (1994).

[12]L. Havela, V. Sechovský, Y. Aoki, Y. Kobayashi, H. Sato, K. Prokeš, M. Mihálik, and A. A. Menovsky, J. Appl. Phys. **81**, 5778 (1997).

[13]A. Ya. Perlov, P. M. Oppeneer, V. N. Antonov, A. N. Yaresko, and B. Yu.Yavorsky, J. Alloys Compd. **271**, 486 (1998).

[14]L. Havera, V. Sechovsky, K. Prokes, H. Nakotee, E. Brück, and F. R. de Boer, J. Alloys Compd. **207-208**, 249 (1994).

[15]A. Wölfel, L. Li, S. Shimomura, H. Onodera, and S. van Smaalen, Phys. Rev. B **82**, 054120 (2010).

[16]J. Laverock, T. D. Haynes, C. Utfeld, and S. B. Dugdale, Phys. Rev. B **80**, 125111 (2009).

[17]T. Sato, S. Souma, K. Nakayama, T. Takahashi, S. Shimomura, and H. Onodera, J. Phys. Soc. Jpn. **79**, 044707 (2010).

[18]M. Mizumaki, N. Kawamura, and H. Onodera, Phys. Status Solidi C **3**, 2767 (2006).